Jeong, Y., Nakagawa, H., Shimada, H., Matsui, K., Kim, J., On the underground imaging using borehole camera.
International Symposium on the Fusion Technology of Geosystem Engineering, Rock Engineering and Geophysical Exploration
Seoul, Korea, Nov. 18-19, 2003

On the underground imaging using borehole camera

Yun-Young Jeong[1], Hideaki Nakagawa[2], Hideki Shimada[1],
Kikuo Matsui[1], JaeDong Kim[3]
[1]Kyushu University, Dept. of Earth Resources and Mining Engineering, Fukuoka, Japan
[2]Kyushu Electric Power Co. Inc., Fukuoka, Japan
[3]Kangwon National University, Dept. of Geosystem Engineering, Chuncheon, Korea

Abstract: It is only possible through the image analysis of borehole wall and the core recovered from borehole constructed in rock mass that the real information about geologic characteristics in rock mass is directly obtained in primary research. Monitoring apparatus with multi-functional utility has implemented and applied in-situ condition for finding the geologic condition of target area. But, this apparatus is very expensive to be applied at the risk of loss during monitoring and cause hard work for moving them to the determined position. This paper shows the underground imaging from the borehole information obtained by a borehole camera with the simple utility and low cost enough to investigate the characteristics of borehole wall. Monitoring for this has been done in open-pit mine located at the northeastern part of Fukuoka Prefecture in Japan, and finally the three dimensional imaging of geological discontinuity was discussed relative to the field condition.

1. Introduction

In the primary survey for engineering practice, many of geophysical and geological methods are utilized for finding information about subsurface geological formations. Core and the image analysis of borehole wall, most of all, play a role of crucial indicator (Rafat et al., 2001). Many kinds of apparatuses have recently been developed for monitoring borehole wall, but this monitoring apparatus with multi-functional utility should have been exposed to the high risk of loss in rock mass caused by the complication of discontinuity net. In this regard, a borehole camera with the simple utility and low cost enough to investigate the characteristics of borehole wall was requested and some kinds of portable type have been invented.

The image of borehole wall provides the basis of the underground imaging which helps a field engineer in his understanding about the subsurface geological formations of target area. There are two interesting studies about the virtual representation of the underground imaging, which focus in the virtual representation using VRML language for restoring a quarry (Pinto et al., 2002) and in mapping of three-dimensional structures of Chimney Rock fault system by integrating air photograph interpretation and differential global positioning system (GPS) location data (Maerten et al., 2001). But there were few attempts to do the three-dimensional imaging of target area in local range.

For an alternative proposal, this paper suggests the three-dimensional imaging using a portable type of borehole camera and the corresponding numerical formulation.

2. Site overview and borehole camera

The target area for field survey was two sites on the second floor of bench in Higashitani mine, which is open-pit limestone quarry with the productivity of the third scale in Japan and located in Kokura-minami Ku, Kitakyushu City, northeastern part of Fukuoka Prefecture, Japan. The second floor of bench is 395 meters above sea level and classified as no weathering zone and weathering zone. Two sites were separately selected from the above two zones and denoted as bench A and bench B respectively.

Bench A is the site of no weathering zone as described in Fig. 1. The dip angle and dip direction of free face was to $70° / 220°$. Traces of many discontinuities appeared in the exposed face of bench. It means that the secondary structure of geological formations had been seriously progressed. Specially, there were two discordant contacts presumed to be the clear trace of intrusion (see the area as like dark column in Fig. 1), which means a sedimentary injection on a relatively large scale.

Bench B is the site of weathering zone as described in Fig. 2. The dip angle and dip direction of free face was to $70° / 220°$, too. Traces of weathering very clearly appeared in the exposed face of bench, but there were not so many traces on the discontinuity presumed to be the secondary structure. It means that there was the serious progress of weathering and so the structural and physical properties of rock were greatly varied.

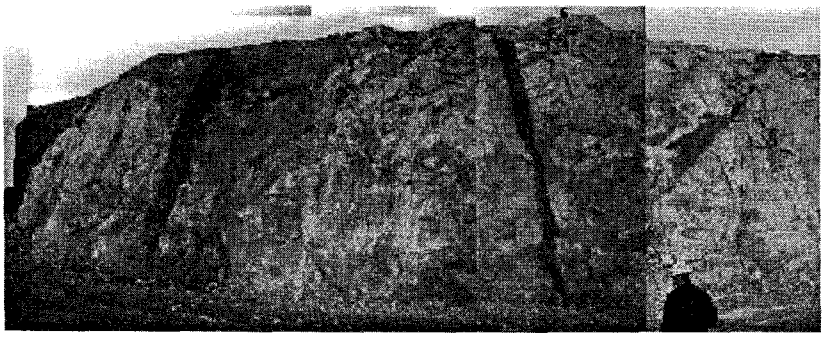

Fig. 1. The front photograph of bench A in no weathering zone.

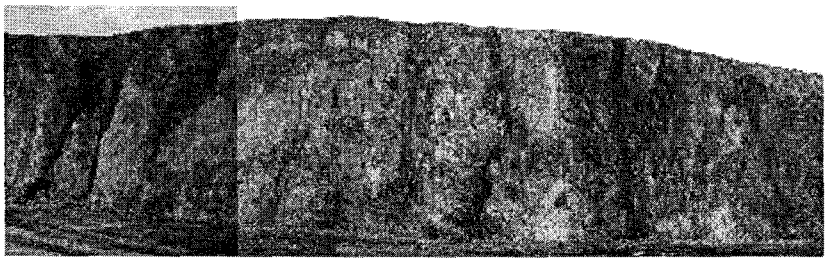

Fig. 2. The front photograph of bench B in weathering zone.

The borehole camera for field survey was the portable borehole camera system invented by Dr. Nakagawa (1999) who is one of the authors of this paper. It has the basic structure consisted of a camera unit, a control unit and a power supply, and also a direction indicator system is included as the simple and useful utility. According to this, the image of side view and a campus type of direction indicator are integrated in the same one image to identify the orientation of discontinuities observed in borehole. The power supply does not require the special and heavy device, and even the battery for starting a car can be used for it.

Another specifications were given in Table 1.

Table 1. Specifications of portable borehole camera system.

Applicable Conditions	Bore size	ϕ 50 mm to 116 mm ϕ 40 mm compatible is optional
	Depth observation	Max. 180 m
	Temperature	0° ~ 40°C
	Borehole direction	All directions
Camera unit		·CCD camera Image pick up device 1/2″ interline system Effective pixels 379392 pixels, Horizontal resolution 470 TV lines Power consumption 3.5 W ·Cable Outside diameter ϕ 11 mm, 9-strand composite cable, approx. 180 m with a measure ·Lens' focal length : 1.2 mm ·Lighting equipment : E-5 bulb, rating 8V
Control unit		·Video cassette recorder with liquid crystal display Recording system : VHS format, Tape to be used : VHS cassette tape Recording time : 9 hours at max. (when T-180 tape, EP mode) Liquid crystal panel : 6.5″ TFT active matrix system Power consumption : Approx. 26W ·Video titler ·Microphone amplifier Rated input power : 5.5 mV (1 kHz with 15V DC), Frequency : 7.0 Hz ~ 40 Hz Gain : 4.0 dB (1 kHz with 15V DC)
Power supply		·The battery included in the control unit ·AC power supply can also be used

3. Three dimensional imaging

Discontinuities classification

Through analyzing the borehole images obtained by the above borehole camera, the following parameters were clearly detected: that are the persistence and width of aperture, the occurrence of filling material, width of the filling, the persistence of discordant contacts, and the orientation of discontinuities. Further, the diameter of borehole was 0.1 m and it was 0.1 m – 100 m that the size range of joints similarly defined in another studies as well as the suggestion by Brekke and Howard (1972). Therefore, detected discontinuities can be considered as joints or another geological structure.

They were classified as 7 types, which are horizontal joints, inclined joints, sub-horizontal joints, open joints, filling, dike and fault. In this paper, horizontal joints are defined for the joint with a dip less than 10° and inclined joints for the joint with a dip of between 10° and 80°. Joints dipping at 20° had to be divided from inclined joints and sub-horizontal joints were termed, because it seems like a true horizontal line in borehole image resulted from the condition that borehole is boring with the inclination of 20°. A clear discordant contact was considered as dike in that there were two discordant contacts presumed to be the clear trace of intrusion on the free face of bench. Two normal faults were detected by the persistence of clear indicators as denoted in Fig. 3.

Fig. 3. A trace of fault with indicators in footwall, hanging wall and fracture plane.

Preconditions

As considering two facts which the first is that discontinuities, appeared on the surface except geological fold, could be described as linear structure, and the second is that on a large scale, rock joints often appear to be planar and, therefore, are not perfect fractals (Brown and Scholz, 1985), it is not true hypothesis to describe the plane of discontinuities as a plat plane. Therefore, a liner algebra equation was implemented for three-dimensional imaging. This numerical formulation and its graphics requested some preconditions.

The coordinate system was based on that depicted in Fig. 4, which it was a right-handed coordinate system and plus direction of y-axis was set to the north of azimuth. Some limitations were requested for inducing the equation of a plane on the plane of discontinuities through the orientation information obtained from the image of borehole wall. As depicted in Fig. 5, the position of borehole was defined as the origin of coordinate and the depth of discontinuities was defined as the length of perpendicular line from it on the surface to any discontinuity, and then the origin of normal vector on the plane of discontinuity was set to the intersection point between the above perpendicular line and any discontinuity.

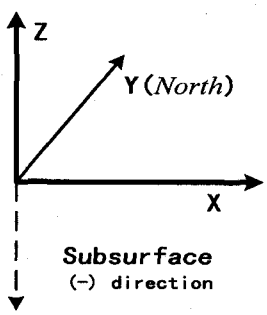

Fig. 4. Suggested coordinate system.

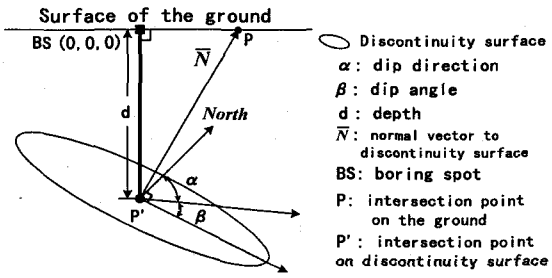

Fig. 5. Summary of the related limitations.

Numerical formulation

According to a mathematical axiom, normal vector of a plane is previously defined and then liner equation of a plane is defined as follows (Boas, 1983)

$$\overline{N} = ai + bj + ck \tag{1}$$

where *a,b,c* is the direction component of each coordinate, *i* is a unit vector for axis x and *j* for axis y and *k* for axis z.

$$a(x - x_o) + b(y - y_o) + c(z - z_o) = 0 \tag{2}$$

where $(x - x_o)$ is the difference vector for axis x and $(y - y_o)$ for axis y and $(z - z_o)$ for axis z.

Through deducing the equation of a plane for discontinuities based on the above preconditions and equation, the general equation was obtained as the function of dip angle, dip direction, and depth.

$$\sin\alpha \sin\beta x + \cos\alpha \sin\beta y + \cos\beta z = -d\cos\beta \tag{3}$$

where β , α is respectively the dip angle and dip direction of discontinuities, d is the absolute value on the depth of discontinuities.

However, if the boring direction of borehole is inclined from the perpendicular direction of borehole position, the depth of discontinuities must be revised according to the azimuth (θ) and degree (γ_z) of inclination. Also, It should be largely classified as two cases, which the value of $(90^\circ - \gamma_z)$ is over and less than the dip angle of discontinuities.

On the first case, $(90^\circ - \gamma_z) \rangle$ *dip angle*, there were two extra conditions denoted in Fig. 6.

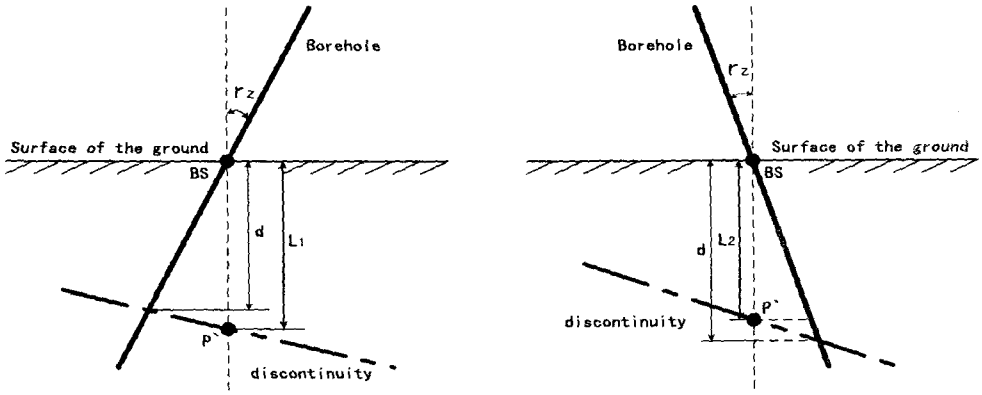

Fig. 6. Two extra conditions on the first case.

In Fig. 6, L_1 and L_2 were respectively defined as follows

$$L_1 = |d|(1 + \tan\gamma_z \tan\beta) \tag{4}$$

$$L_2 = |d|(1 - \tan\gamma_z \tan\beta) \tag{5}$$

By the above definition about depth, the depth (d) of discontinuities becomes to be d or L_1 or L_2 and the three general equations were finally deduced according to the azimuth and degree of borehole inclination.

$$\sin\alpha \sin\beta x + \cos\alpha \sin\beta y + \cos\beta z = -d\cos\beta \tag{3}$$

$$\sin\alpha \sin\beta x + \cos\alpha \sin\beta y + \cos\beta z = -L_1\cos\beta \tag{6}$$

$$\sin\alpha \sin\beta x + \cos\alpha \sin\beta y + \cos\beta z = -L_2\cos\beta \tag{7}$$

On the second case, $(90^\circ - \gamma_z) \leq$ *dip angle*, there were two extra conditions denoted in Fig. 7.

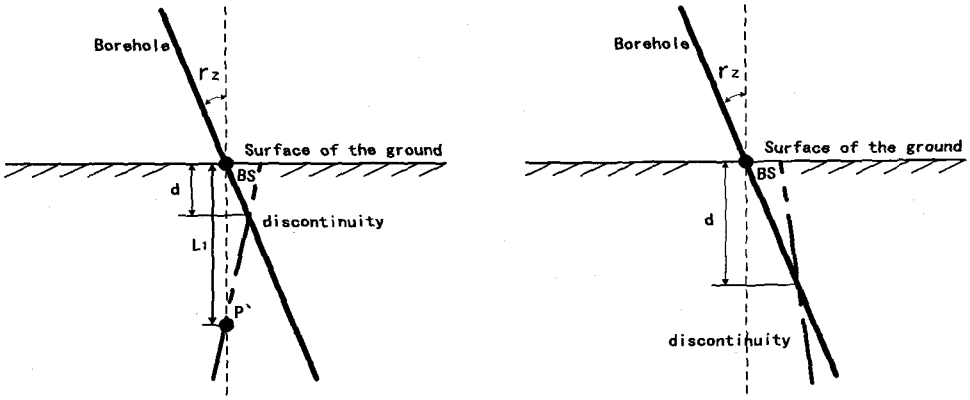

Fig. 7. Two extra conditions on the second case.

The L_1 in left condition in Fig. 7 was defined as the above, but it was found that the right condition happens when discontinuities could not be detected on the perpendicular line of borehole position. The discontinuities coincided with the right condition were excluded, because it does not correspond to the concept of the above preconditions, and were related to the azimuth of borehole inclination as follows.

$$\left|(\theta + 90^\circ) - 360^\circ\right| \; < \; \alpha \; < \; \left|(\theta + 270^\circ) - 360^\circ\right| \tag{8}$$

Therefore, the only two general equations were finally suggested on this case.

$$\sin\alpha \sin\beta x + \cos\alpha \sin\beta y + \cos\beta z = -d\cos\beta \tag{3}$$

$$\sin\alpha \sin\beta x + \cos\alpha \sin\beta y + \cos\beta z = -L_1 \cos\beta \tag{6}$$

4. Imaging result

Through the above formulation, the engineering geological analysis by three-dimensional imaging was actualized and applied to the above two sites, bench A and bench B, which many boreholes were bored with the inclination of 20°. The free face of bench A could be revealed as the simple sketch in Fig. 8 described with the trace assumed as geological intrusion and the clearer linear structure exposed on the face.

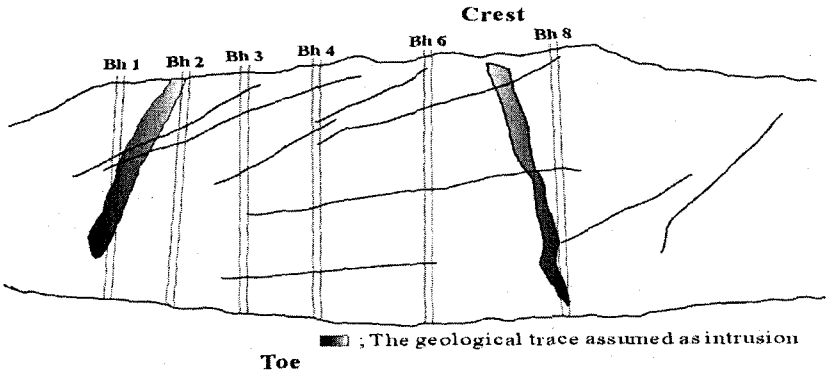

Fig. 8. A simple sketch on bench A.

Through the field survey in this site, it was found that there were the five types of discontinuities, which were inclined joints, open joints, sub-horizontal joints, dike and filling. Inclined joints and filling were described as three-dimensional image in Fig. 9 and Fig. 10, respectively.

In Fig. 9, inclined joints, the largest number of five types, appeared as multiples of random distribution rather than a predominant pattern. It means that this principally relates to the many small traces of discontinuities on free face. In Fig. 10, some fillings with the average width of 4.66 mm were detected in borehole 1, borehole 6 and borehole 8. They can invoke the mechanical weakness, but through the variation of viewpoint on this image, it is found what direction is effectively avoided the effect invoked by their persistence.

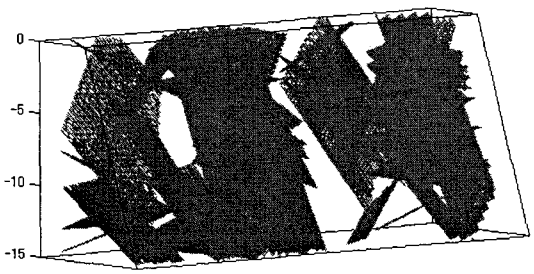

Fig. 9. Three-dimensional image on inclined joints.

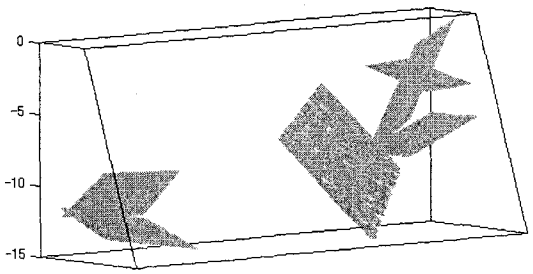

Fig. 10. Three-dimensional image on filling.

All discontinuities, as a general image of bench A, were combined in Fig. 11 with the related coloring, which inclined joints were drawn in gray color, open joints in green color, sub-horizontal joints in gray color, dike in dark red color and fillings in copper color. The viewpoint of this image was set to that corresponding with the above sketch on bench A for the comparison between two images. It is assumed that dikes on boreholes 1, 6 and 8 relate to the geological intrusion exposed on free face, also dike on borehole 4 relate to another intrusion which occurred relatively bellow the toe of bench. Besides, the clearer liner structure on free face did not show the good similarity with the general image. It means that bench A had been largely affected by the blasting by mining or another process.

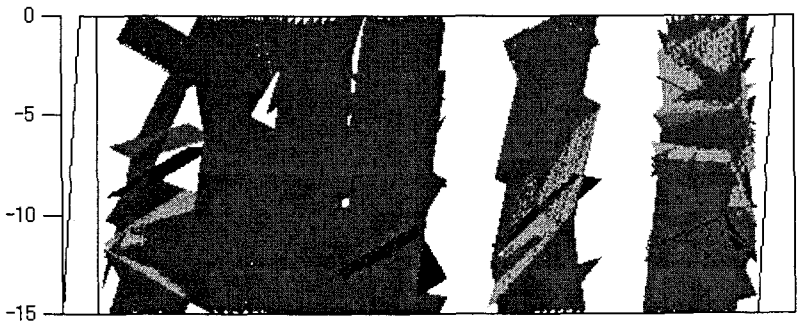

Fig. 11. A general image of bench A.

The free face of bench B could be revealed as the simple sketch in Fig. 12 described with the trace was caused by the development of deep weathering and the clearer linear structure exposed on the face.

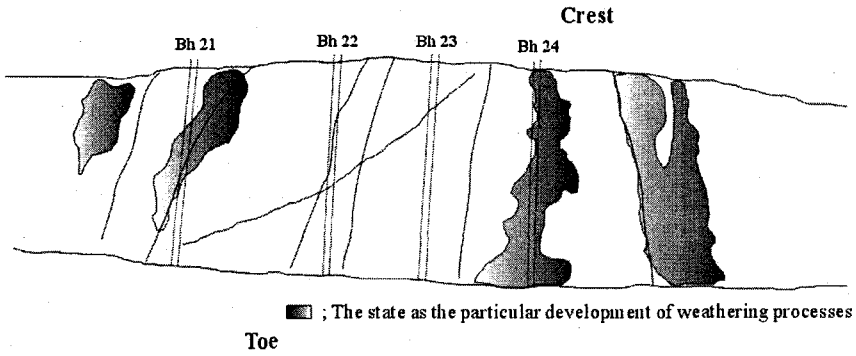

Fig. 12. A simple sketch on bench B.

In bench B, there were the six types of discontinuities, which were inclined joints, horizontal joints, sub-horizontal joints, open joints, fault and filling. Inclined joints, the largest number of six types, and filling were described in Fig. 13 and Fig. 14, respectively.

As seen in Fig. 13, inclined joints mainly appeared in the area of boreholes 22 and 23, which did not show the development of deep weathering. Also, it was found that there was filling in the areas without the development of weathering in Fig. 14.

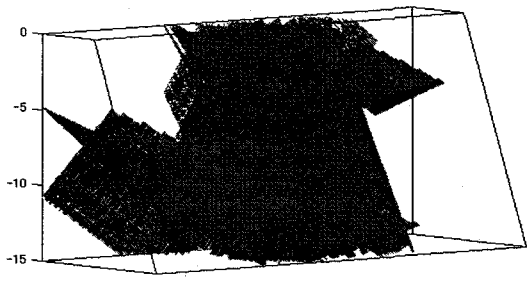

Fig. 13. Three-dimensional image on inclined joints.

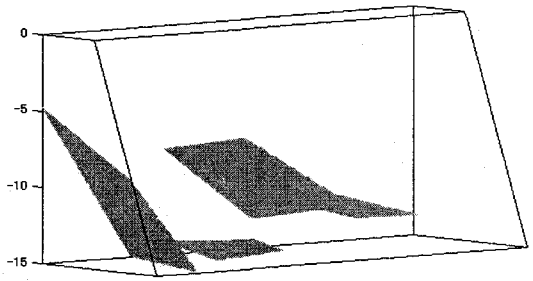

Fig. 14. Three-dimensional image on filling.

All discontinuities, as a general image of bench B, were combined in Fig. 15. The viewpoint of this image was set to the above. Through the comparison with the sketch on bench B, it is assumed that faults drawn in magenta color have the meaning relation with the inclined trace exposed on the area of boreholes 22 and 23, also inclined joints with the nearly vertical trace. Any discontinuities except an inclined joint were not detected in the position of borehole 24. This results from that the position of borehole located in where the development of weathering obviously appeared in free face.

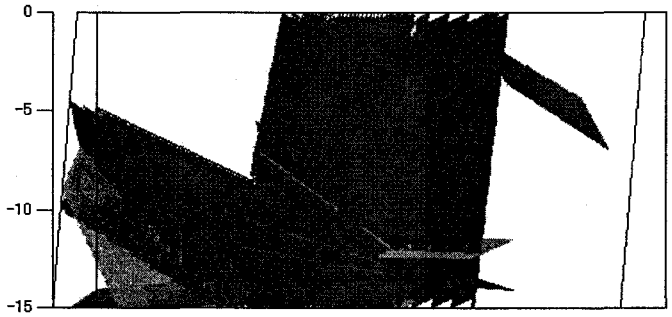

Fig. 15. A general image of bench B.

5. Conclusion

The numerical formulation and corresponding equations were established for the three-dimensional imaging based on the image of borehole wall. This was applied to the two sites, bench A and B, of open pit mine. The three-dimensional images of each bench had two capacities, which is to analyze the trace exposed on free face from the point of engineering geology and to understand visually the distribution of discontinuities within each bench. It gives an engineer the good interface with rock mass that this visualization on the information within borehole can be obtained from the image of a portable type of borehole camera comfortably used in engineering practices.

Therefore, the methodology suggested in this paper shows another tool in the application of rock mass.

Acknowledgements

The authors thank the staff from higashitani-mine for supporting the safety and the good arrangement of process in the field survey. Also, it had been possible to use the related apparatuses of borehole camera from cooperating with Kyushu Electric Power Co. Inc.

References

G. Rafat, B. Lehmann, A. Toumani, H. Rueter, 2001, Characterisation of rock ahead and around tunnels and boreholes by use of geophysical and geological methods, International Journal of Rock Mechanics and Mining Sciences, Vol. 38, 903-908.

V. Pinto, X. Font, M. Salgot, J.C. Tapias, T. Ma$\tilde{n}a'$, 2002, Using 3-D structures and their virtual representation as a tool for restoring opencast mines and quarries, Engineering Geology, Vol. 63, 121-129.

Laurent Maerten, David D. Pollard, Frantz Maerten, 2001, Digital mapping of three-dimensional structures of the Chimney Rock fault system, central Utah, Journal of Structural Geology, Vol. 23, 585-592.

Hideaki NAKAGAWA, Hiroyuki OISHI, Eisaku MURAOKA, 2002, Development and application of portable borehole camera system for geologic survey, Proceedings of International Workshop on Intelligent Mining Systems, Fukuoka City, Japan, 97-102.

Brekke T.L., Howard T. R., 1972, Stability problems caused by seams and faults, Proceedings of the 1st North American Rapid Excavation and Tunneling Conference, Chicago, USA, Vol. 1, 24-41.

Brown SR, Scholz CH, 1985, Broad bandwidth study of the topography of natural rock surfaces, Journal of Geophysical Research, Vol. 90, No. 12, 575-582.

Mary L. Boas, 1983, Mathematical methods in the physical sciences, 2nd, John Wiley & Sons.